

blood

2010 116: 2656-2664
Prepublished online Jul 7, 2010;
doi:10.1182/blood-2009-12-260026

Biodistribution and retargeting of FX-binding ablated adenovirus serotype 5 vectors

Raul Alba, Angela C. Bradshaw, Lynda Coughlan, Laura Denby, Robert A. McDonald, Simon N. Waddington, Suzanne M. K. Buckley, Jenny A. Greig, Alan L. Parker, Ashley M. Miller, Hongjie Wang, Andre Lieber, Nico van Rooijen, John H. McVey, Stuart A. Nicklin and Andrew H. Baker

Updated information and services can be found at:

<http://bloodjournal.hematologylibrary.org/cgi/content/full/116/15/2656>

Information about reproducing this article in parts or in its entirety may be found online at:

http://bloodjournal.hematologylibrary.org/misc/rights.dtl#repub_requests

Information about ordering reprints may be found online at:

<http://bloodjournal.hematologylibrary.org/misc/rights.dtl#reprints>

Information about subscriptions and ASH membership may be found online at:

<http://bloodjournal.hematologylibrary.org/subscriptions/index.dtl>



Biodistribution and retargeting of FX-binding ablated adenovirus serotype 5 vectors

Raul Alba,¹ Angela C. Bradshaw,¹ Lynda Coughlan,¹ Laura Denby,¹ Robert A. McDonald,¹ Simon N. Waddington,² Suzanne M. K. Buckley,² Jenny A. Greig,¹ Alan L. Parker,¹ Ashley M. Miller,³ Hongjie Wang,⁴ Andre Lieber,⁴ Nico van Rooijen,⁵ John H. McVey,⁶ Stuart A. Nicklin,¹ and Andrew H. Baker¹

¹British Heart Foundation Glasgow Cardiovascular Research Centre, University of Glasgow, Glasgow, United Kingdom; ²Department of Haematology, Haemophilia Centre and Haemostasis Unit, Royal Free and University College Medical School, London, United Kingdom; ³Division of Immunology, Infection and Inflammation, Glasgow Biomedical Research Centre, University of Glasgow, Glasgow, United Kingdom; ⁴Division of Medical Genetics, University of Washington, Seattle, WA; ⁵Department of Molecular Cell Biology, Vrije Universiteit Medical Center (VUMC), Amsterdam, The Netherlands; and ⁶Thrombosis Research Institute, London, United Kingdom

A major limitation for adenoviral transduction in vivo is the profound liver tropism of adenovirus type 5 (Ad5). Recently, we demonstrated that coagulation factor X (FX) binds to Ad5-hexon protein at high affinity to mediate hepatocyte transduction after intravascular delivery. We developed novel genetically FX-binding ablated Ad5 vectors with lower liver transduction. Here, we demonstrate that FX-binding ablated Ad5 predominantly localize to the liver and spleen 1 hour after injection; how-

ever, they had highly reduced liver transduction in both control and macrophage-depleted mice compared with Ad5. At high doses in macrophage-depleted mice, FX-binding ablated vectors transduced the spleen more efficiently than Ad5. Immunohistochemical studies demonstrated transgene colocalization with CD11c⁺, ER-TR7⁺, and MAdCAM-1⁺ cells in the splenic marginal zone. Systemic inflammatory profiles were broadly similar between FX-binding ablated Ad5 and Ad5 at low and intermediate doses,

although higher levels of several inflammatory proteins were observed at the highest dose of FX-binding ablated Ad5. Subsequently, we generated a FX-binding ablated virus containing a high affinity Ad35 fiber that mediated a significant improvement in lung/liver ratio in macrophage-depleted CD46⁺ mice compared with controls. Therefore, this study documents the biodistribution and reports the retargeting capacity of FX binding-ablated Ad5 vectors in vitro and in vivo. (*Blood*. 2010;116(15):2656-2664)

Introduction

Of the 54 different adenoviral serotypes isolated to date, adenovirus serotype 5 (Ad5) has been the most commonly used vector in gene therapy clinical trials. This is, in part, due to clear advantages over alternate strategies including the relatively easy manipulation of its viral genome and feasible scale-up production to high titers (up to 10¹³ viral particles (vp)/mL). Nevertheless, Ad5 presents 2 substantial limitations that have required attention to optimize the use of Ad5 in gene therapy. These include the observation that the majority of the human population has pre-existing neutralizing antibodies against Ad5¹⁻³ and the profound liver tropism observed for Ad5 after intravascular delivery.^{4,5} For this reason, fundamental aspects of Ad5 biology need to be further studied to provide safer and target-specific Ad5 gene therapy vectors. The mechanism of Ad5-mediated gene transfer has now been relatively well characterized. In vitro studies have shown that Ad5 and those Ads from subspecies A, C, D, E, and F may use the coxsackievirus and Ad receptor (CAR) as a primary binding receptor.⁶⁻⁹ This interaction occurs via the fiber knob domain with subsequent interaction of the Ad5 penton base with cellular integrins ($\alpha\beta 3$ and $\alpha\beta 5$), mediating capsid internalization.^{10,11} Although CAR and integrin-binding ablated mutant Ad vectors show a substantial reduction in transduction in vitro, these vectors still predominantly transduce hepatocytes in vivo after intravascular administration.^{12,13}

Injection of Ad5 into the bloodstream leads to a complex series of interactions that impact on the resulting biodistribution and tropism of the virus. It has been demonstrated that Ad5 vectors can interact with a variety of blood cells including neutrophils,¹⁴ platelets,¹⁵ red blood cells,^{2,16-18} macrophages (including Kupffer cells in the liver¹⁹ and macrophages in the spleen²⁰), as well as circulating soluble factors including complement factors,^{21,22} neutralizing antibodies³ and coagulation factors.²³⁻²⁷ A number of recent studies have focused on the role of coagulation factors in defining the tropism of adenoviruses in vivo.^{24,26,27} Originally, factor (F)IX and complement 4 binding protein (C4BP) were shown to interact with fiber knob to bridging the Ad capsid to the hepatocyte cell surface.²³ Subsequently it was demonstrated that vitamin K-dependent coagulation factors FVII, FIX, FX and protein C all possessed the ability to enhance adenoviral tropism in vitro at physiologic levels.²⁴ Using a warfarin-pretreatment model, we demonstrated that FX was the only coagulation factor able to rescue liver gene transfer in warfarin-treated mice.^{25,26}

We recently demonstrated that FX binds at high affinity (~ 2nM) to the Ad5 hexon protein through interaction with the hyper-variable regions (HVRs) on the Ad5 hexon and that this interaction mediates hepatocyte transduction in vivo.²⁶ The γ -carboxyglutamic acid (Gla) domain of FX binds to the hexon

Submitted December 18, 2009; accepted June 20, 2010. Prepublished online as *Blood* First Edition paper, July 7, 2010; DOI: 10.1182/blood-2009-12-260026.

The online version of this article contains a data supplement.

The publication costs of this article were defrayed in part by page charge payment. Therefore, and solely to indicate this fact, this article is hereby marked "advertisement" in accordance with 18 USC section 1734.

© 2010 by The American Society of Hematology

protein through HVRs and the serine protease domain of FX bridges the capsid to cell receptors.²⁶ Heparan sulfate proteoglycans have been shown to have a role on in vivo Ad5 liver transduction,²³ thus suggesting its presence on hepatocytes cell surface. Using 23Å cryo-electron microscopy resolution and modeling based on existing crystallographic data, we identified the contact regions between the FX Gla domain and Ad5-hexon.²⁷ We used this model to engineer novel Ad5 vectors with refined mutations in the Ad5 hexon and assessed their effect on FX binding and FX-mediated gene transfer in vitro and in vivo at low dose (1×10^{10} vp/mouse). We showed that HVR5 and, more importantly, HVR7 manipulation reduced FX binding as evidenced by surface plasmon resonance (SPR) studies and reduced in vitro and in vivo gene transfer to liver.²⁷

Here, we performed detailed in vivo studies at increasing doses of mutant Ad5 vectors in mice, because liver transduction is a nonlinear process, involving vector entrapment, macrophage scavenging and hepatocyte transduction.^{5,19,20} We report the detailed liver and spleen uptake of mutant viruses at increasing doses and demonstrate the substantial effect of FX-binding ablation on biodistribution and gene transfer from Ad in vivo. In addition, we provide a detailed study of the inflammatory profiles of these vectors and the utility of FX-binding ablated Ad5 vectors for retargeting in vivo through incorporating a high affinity CD46 interacting fiber.²⁸

Methods

Vector generation and amplification

Ad5 and hexon-modified Ad vectors were generated by homologous recombination as previously described.²⁷ Ad5-CTL, Ad5-KO1, Ad5-PD1, and Ad5-KO1PD1 were kindly provided by Sue Stevenson²⁹ and Ad35Luc by Jerome Custers (Crucell, The Netherlands). The Ad35 fiber (F35⁺⁺), including 2 amino acid changes (D207G and T245A), was cloned into pAd5CMVlacZ-HVR5*7*E451Q backbone. See supplemental Methods (available on the *Blood* Web site; see the Supplemental Materials link at the top of the online article) for the detailed cloning strategy. Adenoviruses were amplified in our laboratory following the previously described methodology.²⁷ Adenoviral particle titers were calculated by determining protein concentrations using the micro-bicinchoninic acid (BCA) Protein Assay kit (Thermo Scientific) followed by titer calculations using the formula $1 \mu\text{g protein} = 4 \times 10^9 \text{ vp}$.³⁰

In vivo methods

All animal procedures were approved by the United Kingdom Home Office. Male MF1 outbred mice aged between 7 and 9 weeks (Harlan) were used for in vivo experiments. CD46 transgenic mice were obtained as previously described.³¹ Clodronate liposomes (<http://clodronateliposomes.org>; 200 μL) were injected into the tail vein 48 hours prior to adenovirus administration as previously described.²³ X-bp treated animals were injected with 4.8 mg/Kg X-bp 30 minutes before injection of the virus as previously described.²⁶ Adenoviral titers used in this experiment were: Ad5: 3.2×10^{12} vp/mL; 1.9×10^{11} plaque-forming units (pfu)/mL, vp/pfu: 16.9; Ad5-HVR5*7*E451Q: 4.3×10^{12} vp/mL; 1.3×10^{11} pfu/mL; vp/pfu: 34.4; Ad5-HVR5*7*E451Q/F35⁺⁺: 1.2×10^{12} vp/mL; 2.5×10^{10} pfu/mL; vp/pfu: 47.2. All animals experiments were performed with a minimum $n = 5$. Statistical analysis was generated using the unpaired Student *t* test with statistical significance accepted at $P < .05$.

β -Galactosidase transduction profiles in liver and spleen

β -Galactosidase transgene expression was analyzed using β -Gal enzyme-linked immunosorbent assay (ELISA) kit (Roche) according to the manufacturer's instructions. Liver lobes and spleens were fixed in 2% paraformal-

dehyde for 16 hours at 4°C and stained for β -galactosidase activity in 5-bromo-4-chloro-3-indolyl- β -D-galactoside (X-gal) staining solution [0.1 M phosphate buffer, pH 7.3, 2 mM MgCl₂, 5 mM K₃F₃(CN)₆, 5 mM K₄Fe(CN)₆, and 1 mg/mL X-gal] at 37°C overnight.

Viral genome content of liver and spleens

DNA was extracted from tissues using the QIAamp DNA mini kit (QIAGEN) following the manufacturer's instructions. DNA was quantified using Nanodrop spectrophotometer (ThermoScientific) and 100 ng of DNA containing viral genomes were quantified using SyBR green real-time polymerase chain reaction (PCR; 7900HT Sequence Detection System; Applied Biosystems) using a concentration of 0.2 μM hexon primers.²⁷

Immunohistochemistry in liver and spleen

Paraformaldehyde fixed, paraffin tissue sections (3 μm) were deparaffinized and rehydrated through an alcohol gradient before incubation with rabbit anti- β -galactosidase antibody (8.4 $\mu\text{g/mL}$; MP Biomedicals) or matched rabbit IgG nonimmune control (8.4 $\mu\text{g/mL}$; Invitrogen) then detected with biotinylated universal secondary antibody (7.5 $\mu\text{g/mL}$, Vector), ABC kit (Vector), and standard diaminobenzidine (DAB) staining and counterstained with hematoxylin or nuclear fast red. For frozen sections, spleens were embedded in Optimal Cutting Temperature medium (O.C.T.)-containing cryomolds (Tissue-Tek), and frozen at -80°C immediately after necropsy. To assess the effect of clodronate liposomes on various splenocyte cell populations, 6 μm spleen sections from phosphate-buffered saline (PBS) control groups $-/+$ clodronate treatment were analyzed by immunohistochemistry using antibodies for the following markers: F4/80, MARCO, CD169, SIGNR1, CD11b, CD11c, and B220 (see Table 1). Isotype matched controls were used at the same final concentrations (Table 1). Viral transgene expression (*Escherichia coli* β -galactosidase) was detected 48 hours after injection using a rabbit anti- β -galactosidase polyclonal antibody (MP Biomedicals LLC) in combination with SIGNR1, CD11b, CD11c, B220, reticular fibroblast marker (ER-TR7), and MAD-CAM-1. Frozen sections were fixed using either ice-cold acetone or 4% paraformaldehyde, sections rinsed in PBS and blocked for 30 minutes in 10% normal goat serum (Vector Laboratories). Primary antibodies were incubated simultaneously for 1 hour at room temperature. Secondary antibodies were diluted 1:500-1:750 in PBS + Tween 0.05% with 2% normal goat serum and incubated for 1 hour at room temperature. Slides were mounted with ProLong Gold+DAPI (Invitrogen). Immunofluorescence was captured using an Olympus BX60 fluorescence microscope (10 \times objective) and images acquired using Cell software (Olympus). Monochrome images (1200 pix \times 1600 pix = 885 \times 1180 μm with a 10 \times objective) were acquired through fluorescence filters for FITC and TRITC using an Olympus BX60 fluorescence microscope (10 \times objective) at room temperature. Images were acquired and merged using Cell software (Olympus). Images were processed to reduce background using ImageJ (National Institutes of Health). Adjustments were applied equally to all compared images.

Cytokine and chemokine analysis

See supplemental Methods.

SPR analysis

Binding analysis was performed using a Biacore T100 (GE Healthcare). FX (455 RU) and CD46 (542 RU) were covalently immobilized onto the flowcell of a CM5 biosensor chip by amine coupling according to the manufacturer's instructions. Subtracted sensorgrams were generated by subtracting the signal from a surface subjected to a blank amine immobilization. Virus (10^{11} VP/mL) in 10 mM HEPES pH 7.4; 150 mM NaCl; 5 mM CaCl₂; 0.05% Tween 20 was passed over the chip at a flow rate of 30 $\mu\text{L}/\text{minute}$.

Table 1. Antibodies used for IHC-Fr

Antibody specificity	Isotype	Fixation	Clone	Final conc.	Source	Secondary antibody
β -galactosidase (<i>Escherichia coli</i>)	rabbit IgG ₁	Acetone/4% PFA		8.3 μ g/mL	MP Biomedical	Gt α -Rb IgG Alexa488
B220 (CD45R)	rat IgG _{2a} , κ	4% PFA	RA3-6B2	1.25 μ g/mL	eBiosciences	Gt α -Rt IgG Alexa488/546
CD11b	rat IgG _{2b} , κ	Acetone	M1/70	0.5 μ g/mL	Abcam	Gt α -Rt IgG Alexa488/546
CD11c (α X β 2 integrin)	Ar hamster IgG	Acetone	N418	2.5 μ g/mL	Abcam	Gt α -Ham IgG Alexa488/546
CD169 (Sialoadhesin)	rat IgG _{2a}	4% PFA	Moma-1	0.5 μ g/mL	Bachem	Gt α -Rt IgG Alexa488
CD209b (SIGNR1)	rat IgM	4% PFA	ER-TR9	4 μ g/mL	Abcam	Gt α -Rt IgM Alexa488/594
F4/80 (M Φ)	rat IgG _{2a}	4% PFA	Cl:A3-1	20 μ g/mL	Abcam	Gt α -Rt IgG Alexa488
MAdCAM-1 (mucosal vascular addressin-1)	rat IgG _{2a} , κ	Acetone	MECA-367	10 μ g/mL	eBiosciences	Gt α -Rt IgG Alexa488/546
MARCO (SR-A)	rat IgG ₁	4% PFA	ED31	2 μ g/mL	Bachem	Gt α -Rt IgG Alexa488
Reticular fibroblast and fibres Ab	rat IgG _{2a}	4% PFA	ER-TR7	1 μ g/mL	Abcam	Gt α -Rt IgG Alexa488

Antibodies used in this study are listed alphabetically. Isotype controls were as follows: rabbit IgG₁ (Vector Laboratories); rat IgG_{2a} (Abcam); rat IgG_{2b} (Abcam); Armenian hamster IgG (eBiosciences); rat IgM (Abcam); and rat IgG₁ (Vector Laboratories).

IHC-Fr indicates immunohistochemistry frozen; CD, cluster of differentiation molecule; M Φ , macrophage; SIGNR1, specific ICAM3 grabbing nonintegrin related-1; SR-A; scavenging receptor A; Ab, antibody; IgG, immunoglobulin G; Ar Ham, Armenian hamster; IgM, immunoglobulin M; PFA, paraformaldehyde; Gt, goat; Rb, rabbit; and Rt, rat.

Results

We recently generated a series of hexon-modified Ad5 vectors with point mutations or selected HVR loop “swaps” in HVR5 and HVR7 for the respective regions of the Ad26 hexon, that do not bind FX.²⁷ Table 2 describes the hexon modifications incorporated. All hexon-modified Ad5 vectors including HVR swaps and incorporating several mutations displayed reduced liver transduction after intravenous delivery of 1×10^{10} vp per mouse.²⁷ In addition, at the same dose, intramuscular injection (tibialis anterior) of Ad5 and Ad5-HVR5*7*E451Q showed no difference on transduction profiles in mice (supplemental Figure 1). As defined previously, liver transduction is a nonlinear and highly dose-dependent process.⁵ Therefore, we sought to further evaluate liver transduction under defined conditions.

Liver transduction by hexon-modified vectors in macrophage-depleted mice after high-dose viral administration

To characterize the effect of Ad5-hexon modification on liver gene transfer, we studied the effect of high-dose viral administration in macrophage-depleted mice. Liver sinusoidal macrophages (Kupffer cells) efficiently clear intravenously administered Ad reducing liver gene transfer.⁵ Intravenous injection of clodronate liposomes has been shown to deplete Kupffer cells as well as macrophage subpopulations in the spleen, lung, lymph nodes, joints, and testis.^{19,32} Macrophage-depleted MF1 mice were intravenously injected with 1×10^{11} vp/mouse and killed 48 hours later. Al-

though Ad5 efficiently transduced the liver, no detectable liver transduction was observed for Ad5-HVR5(Ad26), Ad5-HVR7(Ad26), or Ad5-HVR5 + 7(Ad26) at high doses (Figure 1). Consistent with previous results,²⁷ a low level of liver transduction was observed in mice injected with Ad5-HVR5* (Figure 1). However, no liver transduction was observed in mice injected with Ad5-HVR7*, the Ad5-E451Q point mutant or Ad5-HVR5*7*E451Q, indicating that point mutations introduced in HVR7 have a substantial impact on liver transduction.²⁷ Therefore, Ad5-HVR7(Ad26) and Ad5-HVR5*7*E451Q were selected for further detailed studies.

Biodistribution of FX-binding ablated Ad5 vectors at early (1 hour) and late (48 hours) time points

Toxicity and hence safety and efficacy of Ad vectors in the setting of intravenous delivery are dictated by early biodistribution and subsequent gene transfer. We therefore performed a series of experiments quantifying viral genomes in various tissues at an early time point after injection (1 hour) with Ad5 or Ad5-HVR5*7*E451Q. Macrophage-depleted mice treated with clodronate liposomes (CL+) or control mice (CL-) were injected intravenously with high-dose Ad (1×10^{11} vp/mouse) and killed 1 hour after injection (Figure 2). Ad5 levels in the liver and spleen at 1 hour after injection were unaffected by macrophage depletion (Figure 2). However, Ad5 levels in the liver were substantially higher than in the spleen. For FX-binding ablated Ad5-HVR5*7*E451Q, a different distribution profile was observed.

Table 2. Hexon modifications introduced in FX-binding ablated Ad5 vectors

Virus nomenclature	Promoter and transgene	Hexon modification
Ad5	CMVlacZ	Wild-type Ad5
Ad5-HVR5(Ad26)	CMVlacZ	Ad5HVR5 swapped for Ad26
Ad5-HVR7(Ad26)	CMVlacZ	Ad5HVR7 swapped for Ad26
Ad5-HVR5+7(Ad26)	CMVlacZ	Ad5HVR5+7 swapped for Ad26
Ad5-HVR5*	CMVlacZ	HVR5 (T270P and E271G)
Ad5-HVR7*	CMVlacZ	HVR7 (I421G, T423N, E424S, L426Y)
Ad5-E451Q	CMVlacZ	HVR7(E451Q)
Ad5-HVR5*7*E451Q	CMVlacZ	HVR5 (T270P and E271G) and HVR7 (I421G, T423N, E424S, L426Y and E451Q)

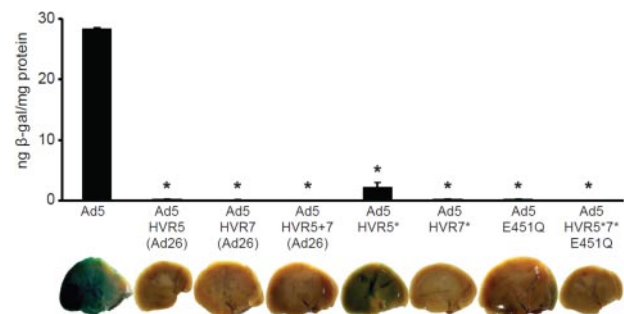


Figure 1. Liver transduction of hexon modified Ad5 vectors using 1×10^{11} vp per mouse. β -galactosidase transgene expression of Ad5 and hexon modified adenoviral vectors after high-dose administration of Ad to macrophage-depleted mice. Animals were killed 48 hours after injection and livers harvested for analysis. (* $P < .0001$ vs Ad5, $n = 5$).

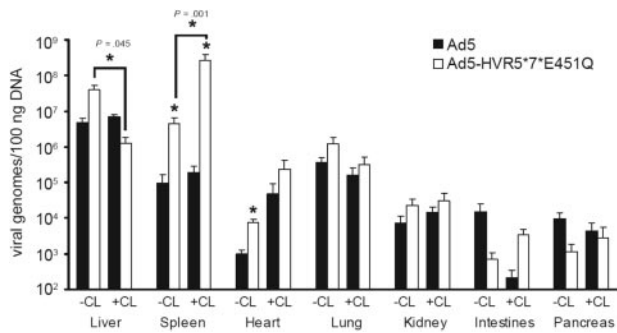


Figure 2. Viral genome content of control and FX-binding ablated Ad vectors at high dose at an early time point. Viral genome content of liver, spleen, heart, lung, kidney, intestines and pancreas tissue 1 hour after the administration of 1×10^{11} vp of Ad5 and Ad5-HVR5*7*E451Q in control (CL-) or macrophage-depleted mice (CL+). DNA was extracted from all tissues and viral genomes quantified using quantitative PCR. (* $P < .05$ vs Ad5, $n = 5$).

After macrophage depletion, levels of Ad5-HVR5*7*E451Q in the liver were significantly reduced, but substantially increased in the spleen (Figure 2). Of note, levels of Ad5-HVR5*7*E451Q in the spleen were substantially higher than Ad5 in both control and macrophage-depleted mice (Figure 2). No statistically significant differences in viral genome content were observed between Ad5 and Ad5-HVR5*7*E451Q in the lung (Figure 2). Although we observed higher levels of FX-binding ablated Ad genomes in the hearts of control mice, the levels were not significantly different to macrophage-depleted mice (Figure 2). In comparison to liver and spleen, lower levels were detected in kidney, pancreas and intestines in control and macrophage-depleted mice administered with Ad5 or Ad5-HVR5*7*E451Q (Figure 2). To further define the biodistribution of these vectors at late time points, we analyzed the viral genome content in the liver and spleen 48 hours after injection with increasing doses of Ad, using titers both higher and lower than the reported nonlinear dose range for Ad5 in mice.⁵ For Ad5, as expected, we observed an increase in liver genome accumulation with increasing doses (Figure 3A). However, liver levels of Ad5-HVR7(Ad26) and Ad5-HVR5*7*E451Q were significantly lower at all doses compared with Ad5 (Figure 3A). Although macrophage depletion increased the quantity of Ad genomes in the liver after Ad5 administration, we observed no effect on the quantity of liver genomes for either Ad5-HVR7(Ad26) and Ad5-HVR5*7*E451Q (Figure 3A). We next assessed splenic uptake of each virus. Interestingly, significantly higher levels of viral genomes were detected in spleens from mice injected with Ad5-HVR5*7*E451Q compared with Ad5 at the highest dose (Figure 3B). This phenomenon was, however, only observed in macrophage-depleted mice administered with a high dose of virus (Figure 3B), suggesting that the macrophage-mediated clearance of viral particles significantly reduces splenic accumulation of intravenously administered Ad regardless of FX-hexon interaction. We also observed an increase in splenic uptake of Ad5-HVR7(Ad26) although these levels were not statistically different ($P = .36$) from those observed for Ad5 (Figure 3B).

Effect of macrophage depletion on transduction profiles of FX-binding ablated Ad5 vectors

We next quantified the level of gene transfer at 48 hours. As expected, with Ad5-HVR7(Ad26) and Ad5-HVR5*7*E451Q we observed significantly reduced liver transduction at all doses compared with Ad5, regardless of macrophage depletion (Figure 4A and supplemental Figure 2A). Consistent with the viral genome

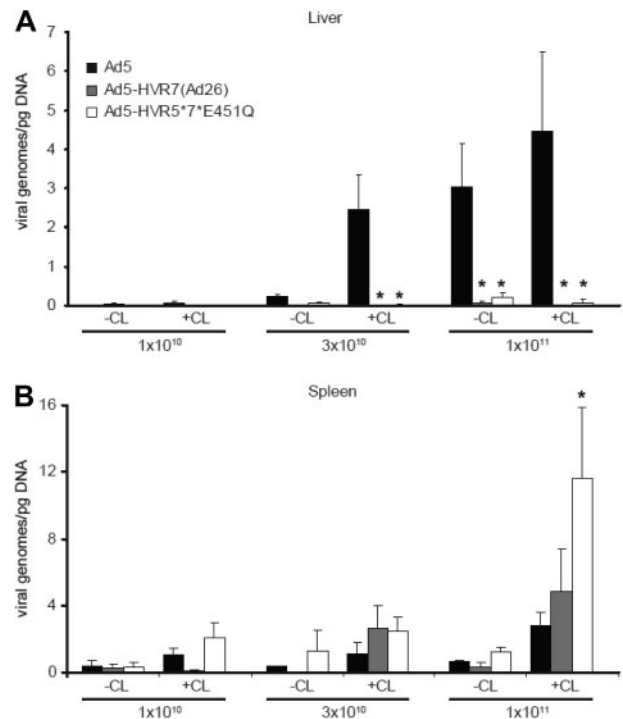


Figure 3. Viral genome content of control and FX-binding ablated Ad vectors 48 hours after administration. Viral genome content of liver (A) and spleen (B) from control (CL-) or macrophage-depleted (CL+) mice 48 hours after injection with increasing doses of Ad5, Ad5-HVR7(Ad26), or Ad5-HVR5*7*E451Q. Ad genomes were detected in liver and spleen after DNA extraction and analysis performed by quantitative PCR. (* $P < .05$ vs Ad5, $n = 5$).

profiles in these animals (Figure 3A-B), higher levels of spleen transduction were observed in mice injected with the highest dose of FX-binding ablated Ad compared with Ad5 (Figure 4B). This increase was only statistically significant in macrophage-depleted mice (Figure 4B and supplemental Figure 2B). Although the increase in the spleen levels of Ad5-HVR7(Ad26) viral genomes were not significantly different, significantly higher levels of splenic transduction were observed. Liver and spleen transduction profiles were corroborated by staining in whole tissues (supplemental Figure 2A-B). Compared with Ad5, lower levels of lung and heart transduction were also observed in mice administered with Ad5-HVR7(Ad26) and Ad5-HVR5*7*E451Q at high doses in macrophage-depleted mice, although the values obtained were substantially lower than those observed for liver and spleen (Figure 4C-D). Collectively, these results indicate that these vectors have inherent splenic tropism at high doses in line with the results presented in Figures 2 and 3.

To further evaluate the effect of FX binding ablation on Ad5 gene transfer in other species, we also analyzed the transduction and viral genome accumulation of intravenously administered FX binding-ablated Ad5 vectors in Brown Norway rats. Transduction and viral genome accumulation data showed Ad5-HVR5*7*E451Q presented a similar biodistribution profile in Brown Norway rats to that observed in MF1 mice, with a significant increase in spleen transduction in the presence of macrophage depletion and ablated liver transduction and viral genome accumulation at the 48-hour time point (supplemental Figure 3).

Localization of transgene expression in liver and spleen

To visualize the cell types transduced by Ad5-HVR5*7*E451Q, immunohistochemical analysis of β -galactosidase expression was

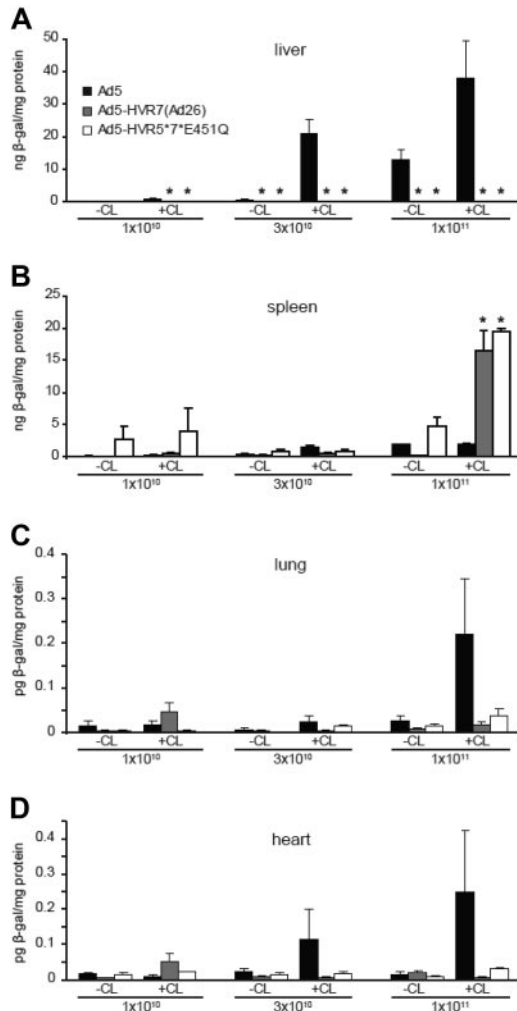


Figure 4. Transduction profiles of Ad5, Ad5-HVR7(Ad26), and Ad5-HVR5*7*E451Q in control (CL-) or macrophage-depleted (CL+) mice. β-galactosidase expression was quantified by ELISA and normalized to total protein content. Animals were killed 48 hours after injection and liver and spleen were harvested for analysis. Liver (A), spleen (B), lung (C), and heart (D) transduction profile at increasing doses (1×10^{10} , 3×10^{10} , and 1×10^{11} vp/mouse; * $P < .05$ vs Ad5, $n = 5$).

carried out in livers and spleens of macrophage-depleted or control mice 48 hours after injection at increasing doses (1×10^{10} , 3×10^{10} , and 1×10^{11} vp) of Ad5 or Ad5-HVR5*7*E451Q. Significant levels of hepatocyte transduction were observed in liver sections from mice injected with Ad5, regardless of macrophage depletion (Figure 5). Conversely, no hepatocyte transduction was observed in liver sections from mice injected with Ad5-HVR5*7*E451Q (Figure 5). We did not observe any transduced cells in any liver section analyzed from any of the Ad5-HVR5*7*E451Q-injected animals under any condition (Figure 5). In the spleen, low levels of transduction of marginal zone cells were observed in sections from mice injected with Ad5, although only at the highest dose of vector (Figure 5). Low levels of marginal zone cell transduction were also observed in spleen sections from mice injected with Ad5-HVR5*7*E451Q (Figure 5). However, in comparison to Ad5, higher levels of marginal zone cell transduction were observed in spleen sections from macrophage-depleted mice injected with Ad5-HVR5*7*E451Q at the highest dose (Figure 5), consistent with the results presented above. The transduced cells appeared to localize entirely around the white pulp in the marginal zone. To identify the virus transgene-expressing

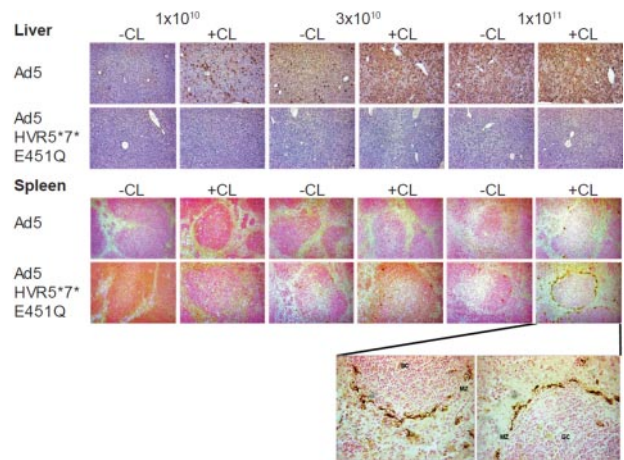


Figure 5. Immunohistochemical analysis of liver and spleen sections. Immunohistochemistry of liver (top panel) and spleen (bottom panel) from macrophage-depleted (CL+) or control mice (CL-) 48 hours after the intravascular administration of 1×10^{10} , 3×10^{10} , and 1×10^{11} vp of Ad5 or Ad5-HVR5*7*E451Q at low magnification (10 \times). Liver transduction was only observed for Ad5, while only Ad5-HVR5*7*E451Q efficiently transduced the spleen at high dose in macrophage-depleted mice. High power magnification (40 \times) of the spleen section at 1×10^{11} vp of Ad5-HVR5*7*E451Q in macrophage-depleted mice is represented below spleen panel. MZ indicates marginal zone; and GC, germinal center.

cell type in the spleen, we first characterized the effect of clodronate liposome pre-treatment on a number of relevant cell populations within the marginal zone of the spleen (F4/80, MARCO, CD169, SIGNR1, CD11b, CD11c, B220, ER-TR7, MAdCAM-1) in PBS-treated animals (supplemental Figure 4). Importantly, we also included structural components (reticular fibroblasts and sinus lining endothelial cells) that are known to be localized within this region of the spleen. The markers that remained detectable within the marginal zone after clodronate treatment (and were therefore available to interact with virus) were selected for colocalization studies. We observed limited or low level colocalization of β-galactosidase expression with SIGNR1⁺, CD11b⁺ and B220⁺ cell types (Figure 6). Moreover, we detected clear colocalization of β-galactosidase expression with CD11c⁺ cells and with structural components of the marginal zone, the reticular fibroblasts (ER-TR7) and MAdCAM-1⁺ sinus lining endothelial cells (Figure 6).

In addition to hexon modification, we analyzed the effect of other capsid modifications on spleen transduction. CAR-binding ablated and integrin-binding ablated Ad5 vectors produced significantly reduced spleen transduction in MF1 mice pre-injected with FX binding protein (X-bp) in the presence of macrophage depletion. Although significant lower levels of transduction were observed in the spleen, CAR-binding ablation, integrin-binding ablation or the combination of both modifications in the parental Ad5 vector were not able to completely preclude spleen transduction after intravenous adenoviral delivery (supplemental Figure 5).

Inflammatory profiles in mice injected with Ad5 and FX-binding ablated vectors

Ad capsid proteins induce innate toxicity after intravascular delivery that elicits the release of different cytokines and chemokines. To analyze the systemic toxicity associated with FX-binding ablated Ad vectors, serum was obtained from mice injected with Ad5 or Ad5-HVR5*7*E451Q 1 hour or 6 hours after administration. Cytokine and chemokine analysis was carried out using a multiplex panel. Serum cytokine/chemokine profiles showed that

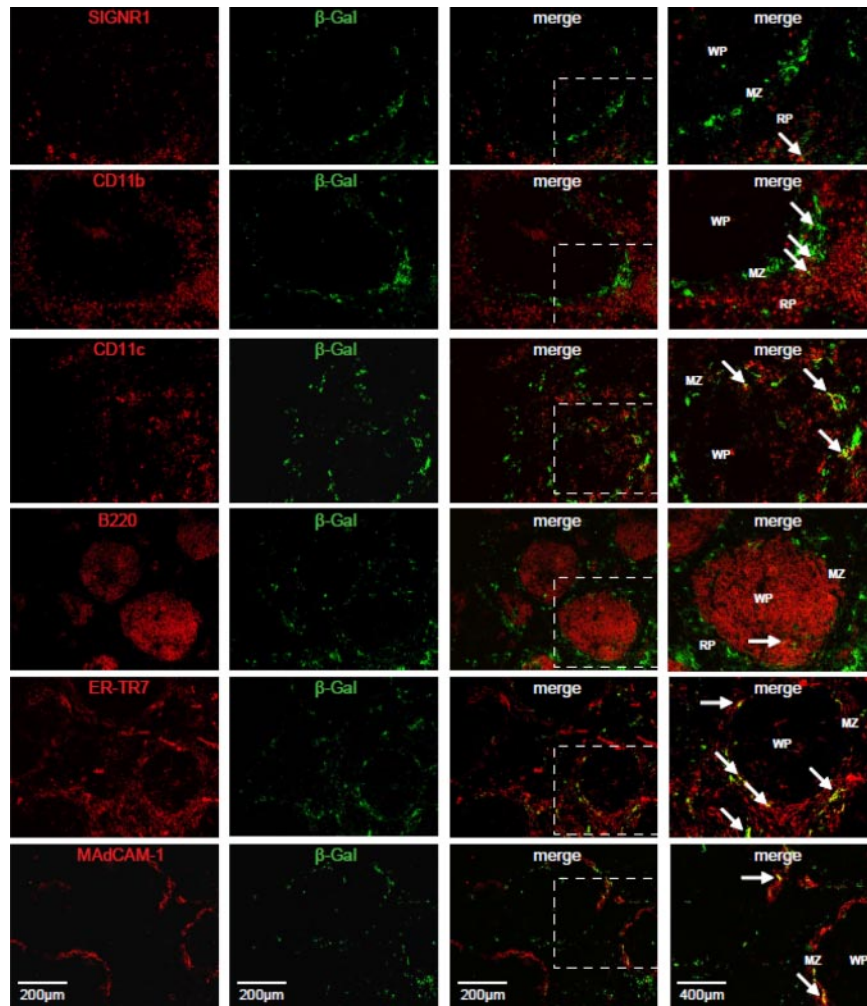


Figure 6. Colocalization of viral transgene expression with spleen cell markers after treatment with clodronate liposomes. Frozen spleen sections (6 μ m) were stained with antibodies for SIGNR1, CD11b, CD11c, B220, ER-TR7, and MAdCAM-1 in combination with an antibody to viral transgene, β -galactosidase (Table 1). Single stained and merged images are presented. An enlarged portion of each merged image is displayed in the far right panel, highlighted by a white box. White arrows indicate regions of colocalization (in yellow). WP indicates White pulp; MZ, Marginal zone, and RP, Red pulp. Images are representative of multiple fields of view from 2-4 different animals.

levels of most inflammatory factors were not significantly different between Ad5 and Ad5-HVR5*7*E451Q after administration of low and intermediate doses (supplemental Table 1). However, at the highest dose we observed an increase in the levels of most cytokines/chemokines on the panel for both Ad5 and Ad5-HVR5*7*E451Q. Comparing Ad5 versus Ad5-HVR5*7*E451Q, we observed a significant increase in interleukin-12 (IL-12), monokine-induced by interferon γ (MIG), and 10-kDa interferon γ -induced protein (IP-10) levels in control and macrophage depleted mice 6 hours after administration of Ad5-HVR5*7*E451Q ($P < .05$; supplemental Figure 6). IL-12, MIG and IP-10 levels were lower in macrophage-depleted mice for both vectors although Ad5-HVR5*7*E451Q induced significantly higher levels of these cytokines and chemokines in both control and macrophage-depleted mice ($P < .05$; supplemental Figure 6). Indeed, we observed higher levels of monocyte chemoattractant protein 1 (MCP-1) and macrophage inflammatory protein 1 α (MIP-1 α) ($P < .05$) with Ad5-HVR5*7*E451Q, but only in macrophage-depleted mice compared with Ad5 (supplemental Figure 6A-B). IL-6 and interferon γ (IFN- γ) cytokines levels have been reported to increase after intravascular delivery of Ad5.³³ In this study, IL-6 levels were similar for Ad5 and Ad5-HVR5*7*E451Q in control mice. However, we observed a significant decrease in IL-6 levels

for Ad5-HVR5*7*E451Q in macrophage-depleted mice compared with control mice (supplemental Figure 6C). In addition, IFN- γ levels did not change between vectors at the highest dose (supplemental Figure 6D). Although we observed significant differences in serum cytokine/chemokine profiles between Ad5 and Ad5-HVR5*7*E451Q, we cannot predict what the associated toxicity for FX-binding ablated Ad in humans will be because the dose that produced changes in inflammatory profiles in mice (4×10^{12} vp/Kg) is significantly higher than doses used in clinical trials.³⁴⁻³⁷

Construction and analysis of a FX-binding ablated Ad5 vector carrying a high affinity fiber from Ad35

To assess the retargeting ability of Ad5-HVR5*7*E451Q, we genetically exchanged the Ad5 fiber for the Ad35 fiber (Ad35⁺⁺) generating Ad5-HVR5*7*E451Q/F35⁺⁺. The F35⁺⁺ gene includes 2 amino acid changes previously described,²⁸ which confers 60 \times higher affinity to CD46 compared with Ad35. To analyze the binding to FX and CD46, we performed SPR experiments using different Ad5 vectors. SPR analysis of the interaction of whole virus to FX immobilized on the sensorchip showed Ad5 could only bind to FX, Ad35Luc to both FX and CD46 while Ad5-HVR5*7*E451Q was not able to bind to FX or

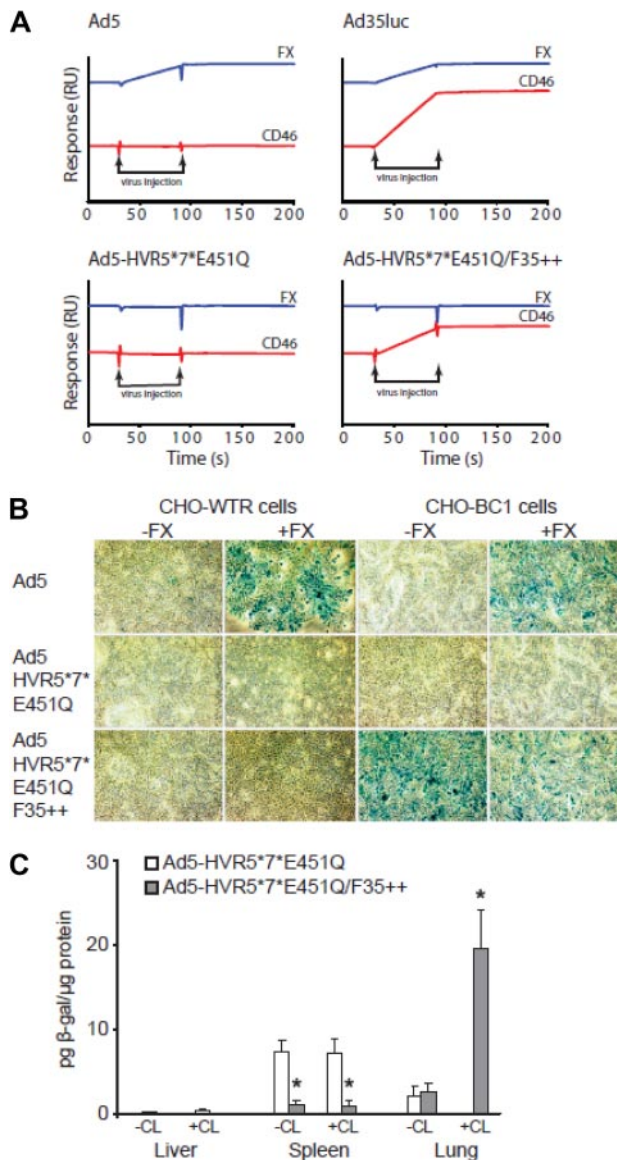


Figure 7. Retargeting of Ad5-HVR5*7*E451Q/F35⁺⁺ to CD46 in vitro and in vivo. (A) Binding analysis was performed by surface plasmon resonance. Flow cell (Fc)1: blank immobilization; Fc2: 542RU CD46; and Fc4 455RU FX were prepared by amine coupling. Viruses at a concentration of 10¹¹ VP/mL were injected across all 4 flow cells at a flow rate of 30 μL/minute in 10 mM HEPES pH 7.4; 150 mM NaCl; 5 mM CaCl₂; 0.005% Tween 20. Representative subtracted sensorgrams (Fc2-Fc1; Fc3-Fc1; Fc4-Fc1) for each virus show the relative change in response (RU). The sensorgrams are off set for easier visualization. (B) Xgal staining of CHO-WTR and CHO-BC1 cells using 1000 viral particles of Ad5, Ad5-HVR5*7*E451Q, and Ad5-HVR5*7*E451Q/F35⁺⁺ vectors in the presence or absence of FX (*P < .05 vs PBS control). (C) Analysis of β-gal transgene expression in the liver, spleen and lung tissue after the intravascular administration of 1 × 10¹¹ vp into CD46 transgenic mice in the presence or absence of macrophage depletion. (*P < .05 vs Ad5-HVR5*7*E451Q, n = 5).

CD46 (Figure 7A). Having demonstrated that the F35⁺⁺ fiber conferred the ability to bind CD46 (Figure 7A), we performed cell binding and transduction experiments in vitro in the presence or absence of FX. In these experiments, we used a cell line stably transfected to express CD46 (CHO-BC1) and a control cell line that does not express this receptor (CHO-WTR). Ad5 bound and transduced both cell types but only in the presence of FX (Figure 7B and supplemental Figure 7A-B) while Ad5-HVR5*7*E451Q was not able to bind or transduce either cell type under these conditions (Figure 7B and supplemen-

tal Figure 7A-B). Of note, Ad5-HVR5*7*E451Q/F35⁺⁺ was able to transduce CHO-BC1 cells in the absence of FX, showing clear retargeting to CD46 (Figure 7B and supplemental Figure 7A-B). To evaluate the potential retargeting of Ad5-HVR5*7*E451Q/F35⁺⁺ in vivo, we injected Ad5-HVR5*7*E451Q or Ad5-HVR5*7*E451Q/F35⁺⁺ into CD46 transgenic mice intravenously in the presence or absence of macrophage depletion. Transduction profiles at 48 hours showed Ad5-HVR5*7*E451Q/F35⁺⁺ transduced the lung in macrophage-depleted mice as previously described,³¹ precluding liver transduction and significantly reducing the levels of spleen transduction compared with Ad5-HVR5*7*E451Q (Figure 7C). In macrophage-depleted CD46 transgenic mice, the lung/liver ratio for Ad5-HVR5*7*E451Q/F35⁺⁺ was ~ 800 (compared with a ratio of ~ 0.05 for Ad5-HVR5*7*E451Q) showing an approximated 16 000-fold increase in lung transduction compared with Ad5-HVR5*7*E451Q. Although we did not observe increased lung transduction in the absence of clodronate liposomes after administration of Ad5-HVR5*7*E451Q, lower levels of spleen and basal liver transduction were observed (Figure 7C). Collectively, these data provide proof of concept for retargeting of FX-binding ablated Ad5 vectors. Nevertheless, strategies will be required to ablate macrophage uptake and fully exploit the retargeting potential of these vectors.

Discussion

Over the past 20 years, virologists and gene therapists alike have sought to elucidate the basic mechanisms used by Ad5 to transduce cells in vivo. Here, we show that vectors ablated for FX-binding display altered biodistribution, tropism and inflammatory profiles compared with parental Ad5 after systemic administration. As previously demonstrated with Ad5,⁵ the dose of vector delivered intravenously can significantly affect liver uptake. In this study, we observed that at all doses studied the levels of liver gene transfer for FX-binding ablated Ad vectors were substantially lower compared with Ad5 in control or macrophage-depleted mice. However, significant differences in splenic uptake and transduction were found. Interestingly, macrophage depletion promoted viral genome accumulation in the spleen after systemic administration of FX-binding ablated vectors at the highest dose used. Despite these substantial differences in biodistribution and tropism, inflammatory profiles were largely unaffected compared with parental Ad5 at low and intermediate doses.

We have previously shown using SPR analysis that neither Ad5-HVR7(Ad26) or Ad5-HVR5*7*E451Q bind to FX²⁷ and we have now further shown purified hexon from these viruses has also undetectable binding to FX (supplemental Figure 8). It is clear from this work and from our previous studies that modulation of HVR7 is required to fully ablate FX binding. Even at substantial viral doses (1 × 10¹¹ vp/mouse), we failed to detect any liver transduction at the cellular level. Therefore, as a vector system to preclude liver transduction, vectors based on the above documented mutations will show considerable promise for liver detargeting purposes. However, our results show that Ad5 vectors devoid of FX-binding still accumulate within macrophages. Previous studies have shown that there is significantly higher accumulation of Ad5 in macrophages of warfarinized mice at early time points (eg, 1 hour) after administration.²² Compared with parental Ad5, we observed a potential increase in viral genome accumulation in the liver 1 hour after

intravenous delivery of FX-binding ablated Ad5. Although this increase was not statistically significant, it suggests that there may be increased uptake of FX-binding ablated Ad5 vectors by Kupffer cells and therefore warrants further investigation.

Importantly, we show that FX-binding ablation affected not only Ad5 biodistribution and liver/spleen transduction but also the transduction of other organs. Of note, lung and heart transduction by FX-binding ablated Ad5 vectors was substantially lower than parental Ad5 at high doses in macrophage-depleted mice (Figure 4C-D). Our data show that although viral genome accumulation in these organs at early time points is not affected by FX-binding ablation, FX-binding may promote adenoviral transduction of certain lung or heart cell populations at the 48-hour time point.

Despite the highly efficient liver detargeting and the lack of transduction in other tissues (lung and heart), we observed important biodistribution and tropism differences for the spleen that may impact on the design and utility of FX-binding ablated vectors. Increased transduction of the spleen by FX-binding ablated vectors only occurs at high dose and only when macrophages are depleted. Of note, the levels of cytokines/chemokines were substantially increased at high dose regardless of macrophage depletion. Our results suggest that FX-binding ablated vectors induce a more robust Th1 immune response than parental Ad5. Macrophage depletion attenuates this response (supplemental Figure 6), indicating that these inflammatory mediators may in part be secreted by macrophages or their secretion induced by macrophage-derived mediators. It is difficult to judge whether the increased Th1 response to FX-ablated vectors would be relevant in the clinical context, as the majority of clinical trials use much lower relative doses of Ad vectors (between $2.5\text{--}7.5 \times 10^{10}$ vp/Kg,³⁴⁻³⁷ compared with our highest dose of 4×10^{12} vp/kg). In our study, we found no differences in spleen transduction or inflammatory responses for the majority of cytokines/chemokines between FX-binding ablated vectors and parental Ad5 at the low or intermediate doses (4×10^{11} vp/Kg or 1.2×10^{12} vp/Kg, respectively). Previous studies have shown that Ad5 can activate macrophages and dendritic cells.³⁸ In addition, Di Paolo and collaborators showed that metallophilic and marginal zone macrophages (CD169⁺ and MARCO⁺ cells) colocalise with Ad vectors in the spleen at early time points after intravascular administration.²⁰ We found significantly greater numbers of β -gal positive cells in the splenic marginal zones after intravenous delivery of FX-binding ablated Ad vectors, but only in macrophage-depleted mice. A number of cell types are known to reside in the marginal zone including metallophilic macrophages, marginal zone macrophages, dendritic cells, fibroblasts, marginal zone B cells and lymphocytes.³⁹ Immunohistochemistry studies showed that the specific transduced cell types found in the marginal zone of the spleen particularly colocalized with CD11c⁺, ER-TR7⁺, and MAdCAM-1⁺. Although we attempted to fully characterize the spleen cell population transduced by Ad5-HVR5*7*E451Q using an extensive range of cell surface markers, the majority of β -gal⁺ cells did not colocalize with single markers, indicating a complex cellular interaction in the spleen mediated by Ad5-HVR5*7*E451Q. Of note, our results indicate that Ad5-HVR5*7*E451Q use FX-independent pathways to transduce splenic cells, perhaps via cell surface interactions with fiber, penton or unmodified hexon regions. Importantly, we found a significant reduction in spleen transduction using CAR-binding or integrin-binding ablated Ad5 vectors. However, these modifications, alone or in combination, did

not completely preclude spleen transduction by Ad5 that suggests multiple mechanisms facilitate spleen uptake and transduction.

Retargeting strategies for Ad5 have been extensively investigated over the past few years (for review see Mebius³⁹ and Alemany⁴⁰). However, most retargeting strategies have not been entirely successful due to the high affinity of the FX-Ad5 complex for hepatocytes.²⁶ The potential for detargeting via FX modulation has been demonstrated by a recent study using an oncolytic version of the HVR5-modified Ad5 vector Ad-GL-HB.⁴¹ The authors showed reduced liver transduction but no decrease in the number of liver viral genomes 5 days after delivery. Although we observed significantly reduced IL-6 induction after administration of Ad5-HVR5*7*E451Q to macrophage-depleted mice, in the Shashkova study IL-6 levels remained high after Ad-GL-HB administration even after viral predosing.⁴¹ These differences could be explained by the fact that the HVR5*7*E451Q mutations completely abolish the interaction with FX²⁷ (supplemental Figure 8) while Ad-GL-HB still is able to bind FX, albeit at a greatly reduced level, and transduces the liver.⁴² Here, we provided a genetic retargeting strategy exchanging the Ad5 fiber for the Ad35⁺⁺ fiber in Ad5-HVR5*7*E451Q and showed efficient retargeting to CD46 in vitro without binding to coagulation FX. In vivo, we observed lung retargeting of Ad5-HVR5*7*E451Q/F35⁺⁺ in macrophage-depleted CD46 transgenic mice with a lung/liver ratio $\sim 16\,000$ times higher than Ad5-HVR5*7*E451Q thereby illustrating the potential of these vectors in future retargeting strategies. However, the retargeting to the lung was only achieved in the presence of macrophage depletion. Additional strategies are still required to manipulate the uptake of Ad5 by macrophages. Therefore, our results indicate that modifications in HVR7 or point mutations included in both HVR5 + 7 have the potential to improve current tumor targeting strategies by increasing liver detargeting and warrant further investigation.

In summary, the present study investigated the biodistribution and tropism of FX-binding ablated Ad5 vectors after intravascular administration. We show that Ad5 vectors devoid of FX binding are not able to transduce hepatocytes regardless of dose or macrophage depletion. Crucially, dosing experiments revealed differences in Ad5 uptake and transduction between FX-binding ablated Ads and parental Ad5, with increased spleen transduction by FX-binding ablated Ads observed only at the highest dose in macrophage-depleted mice. Low levels of transduction observed in other organs indicate a clear splenic tropism for these modified vectors. Therefore, FX-binding ablated Ad vectors in combination with retargeting strategies, offer a new platform for gene therapy applications where evasion of liver gene transfer is required.

Acknowledgments

We thank Nicola Britton and Gregor Aitchison at the British Heart Foundation Glasgow Cardiovascular Research Center (BHF GCRC) for technical assistance, Sue Stevenson for providing the Ad5-CTL, Ad5-KO1, Ad5-PD1, and Ad5-KO1PD1 viruses, and Jerome Custers (Crucell) for the Ad35Luc vector. We thank Paul Garside and James M. Brewer for helpful discussions on spleen immunohistochemistry.

This work was supported by the Biotechnology and Biological Sciences Research Council and British Heart Foundation (A.H.B.). A.M.M. holds a BHF intermediate fellowship. A.L.P. holds a

personal research fellowship from the Royal Society of Edinburgh Scotland Foundation.

Authorship

Contribution: R.A., A.C.B., L.C., R.A.M., S.N.W., S.M.K.B., J.A.G., J.H.M., A.L.P., and A.M.M. performed research; R.A., L.C., S.A.N., J.H.M., and A.H.B. analyzed data; H.W., A.L., and N.v.R. provided essential reagents; R.A. and A.H.B. wrote the

paper and made the figures with S.N.W., A.C.B., L.C., S.A.N., and A.H.B., and all authors edited and agreed; and A.H.B. supervised the project.

Conflict-of-interest disclosure: The authors declare no competing financial interests.

Correspondence: Andrew H. Baker, British Heart Foundation Glasgow Cardiovascular Research Centre, Division of Cardiovascular and Medical Sciences, 126 University Pl, University of Glasgow, Glasgow, G12 8TA, United Kingdom; e-mail: ab11f@clinmed.gla.ac.uk.

References

- Mast TC, Kierstead L, Gupta SB, et al. International epidemiology of human pre-existing adenovirus (Ad) type-5, type-6, type-26 and type-36 neutralizing antibodies: correlates of high Ad5 titers and implications for potential HIV vaccine trials. *Vaccine*. 2010;28(4):950-957.
- Abbink P, Lemckert AA, Ewald BA, et al. Comparative seroprevalence and immunogenicity of six rare serotype recombinant adenovirus vaccine vectors from subgroups B and D. *J Virol*. 2007;81(9):4654-4663.
- Sumida SM, Truitt DM, Lemckert AA, et al. Neutralizing antibodies to adenovirus serotype 5 vaccine vectors are directed primarily against the adenovirus hexon protein. *J Immunol*. 2005;174(11):7179-7185.
- Jaffe HA, Danel C, Longenecker G, et al. Adenovirus-mediated in vivo gene transfer and expression in normal rat liver. *Nat Genet*. 1992;1(5):372-378.
- Tao N, Gao GP, Parr M, et al. Sequestration of adenoviral vector by Kupffer cells leads to a non-linear dose response of transduction in liver. *Mol Ther*. 2001;3(1):28-35.
- Bergelson JM, Cunningham JA, Droguett G, et al. Isolation of a common receptor for Coxsackie B viruses and adenoviruses 2 and 5. *Science*. 1997;275(5304):1320-1323.
- Tomko RP, Xu R, Philipson L. HCAR and MCAR: the human and mouse cellular receptors for subgroup C adenoviruses and group B coxsackieviruses. *Proc Natl Acad Sci U S A*. 1997;94(7):3352-3356.
- Einfeld DA, Brough DE, Roelvink PW, Kovessi I, Wickham TJ. Construction of a pseudoreceptor that mediates transduction by adenoviruses expressing a ligand in fiber or penton base. *J Virol*. 1999;73(11):9130-9136.
- Roelvink PW, Lizonova A, Lee JG, et al. The coxsackievirus-adenovirus receptor protein can function as a cellular attachment protein for adenovirus serotypes from subgroups A, C, D, E, and F. *J Virol*. 1998;72(10):7909-7915.
- Wickham TJ, Mathias P, Cheresh DA, Nemerow GR. Integrins $\alpha_v\beta_3$ and $\alpha_v\beta_5$ promote adenovirus internalization but not virus attachment. *Cell*. 1993;73(2):309-319.
- Nemerow GR, Wickham TJ, Cheresh DA. *The role of $\alpha 5$ integrins in adenovirus infection*. New York: Elsevier Science Publishers; 1993.
- Mizuguchi H, Koizumi N, Hosono T, et al. Car- or αv integrin-binding ablated adenovirus vectors, but not fiber-modified vectors containing RGD peptide, do not change the systemic gene transfer properties in mice. *Gene Therapy*. 2002;9:769-776.
- Koizumi N, Kawabata K, Sakurai F, Watanabe Y, Hayakawa T, Mizuguchi H. Modified Adenoviral Vectors Ablated for Coxsackievirus-Adenovirus Receptor, αv Integrin, and Heparan Sulfate Binding Reduce In Vivo Tissue Transduction and Toxicity. *Human Gene Therapy*. 2006;17:264-279.
- Cotter M, Zaiss A, Muruve D. Neutrophils interact with adenovirus vectors via Fc receptors and complement receptor 1. *J Virol*. 2005;79(23):14622-14631.
- Stone D, Ni S, Yi Li Z, Shayakhmetov D, Lieber A. Intravascular delivery of adenovirus vectors rapidly targets platelets to the reticuloendothelial system. *Mol Ther*. 2006;13(1):S143-S144.
- Nicol CG, Graham D, Miller WH, et al. Effect of adenovirus serotype 5 fiber and penton modifications on in vivo tropism in rats. *Mol Ther*. 2004;10(2):344-354.
- Carlisle RC, Di Y, Cerny AM, et al. Human erythrocytes bind and inactivate type 5 adenovirus by presenting Coxsackie virus-adenovirus receptor and complement receptor 1. *Blood*. 2009;113(9):1909-1918.
- Seiradake E, Henaff D, Wodrich H, et al. The cell adhesion molecule "CAR" and sialic acid on human erythrocytes influence adenovirus in vivo biodistribution. *PLoS Pathog*. 2009;5(1):e1000277.
- Wolff G, Worgall S, van Rooijen N, Song WR, Harvey BG, Crystal RG. Enhancement of in vivo adenovirus-mediated gene transfer and expression by prior depletion of tissue macrophages in the target organ. *J Virol*. 1997;71(1):624-629.
- Di Paolo NC, Miao EA, Iwakura Y, et al. Virus binding to a plasma membrane receptor triggers interleukin-1 α -mediated proinflammatory macrophage response in vivo. *Immunity*. 2009;31(1):110-121.
- Jiang H, Wang Z, Serra D, Frank MM, Amalfitano A. Recombinant adenovirus vectors activate the alternative complement pathway, leading to the binding of human complement protein C3 independent of anti-ad antibodies. *Mol Ther*. 2004;10(6):1140-1142.
- Xu Z, Tian J, Smith JS, Byrnes AP. Clearance of adenovirus by Kupffer cells is mediated by scavenger receptors, natural antibodies, and complement. *J Virol*. 2008;82(23):11705-11713.
- Shayakhmetov DM, Gaggar A, Ni S, Li ZY, Lieber A. Adenovirus binding to blood factors results in liver cell infection and hepatotoxicity. *J Virol*. 2005;79(12):7478-7491.
- Parker AL, Waddington SN, Nicol CG, et al. Multiple vitamin K-dependent coagulation zymogens promote adenovirus-mediated gene delivery to hepatocytes. *Blood*. 2006;108(8):2554-2561.
- Waddington SN, Parker AL, Havenga M, et al. Targeting of adenovirus serotype 5 (Ad5) and 5/47 pseudotyped vectors in vivo: fundamental involvement of coagulation factors and redundancy of CAR binding by Ad5. *J Virol*. 2007;81(17):9568-9571.
- Waddington SN, McVey JH, Bhella D, et al. Adenovirus serotype 5 hexon mediates liver gene transfer. *Cell*. 2008;132(3):397-409.
- Alba R, Bradshaw AC, Parker AL, et al. Identification of coagulation factor (FX) binding sites on the adenovirus serotype 5 hexon: effect of mutagenesis on FX interactions and gene transfer. *Blood*. 2009;114(5):965-971.
- Wang H, Liu Y, Li Z, et al. In vitro and in vivo properties of adenovirus vectors with increased affinity to CD46. *J Virol*. 2008;82(21):10567-10579.
- Smith TA, Idamakanti N, Marshall-Neff J, et al. Receptor interactions involved in adenoviral-mediated gene delivery after systemic administration in non-human primates. *Hum Gene Ther*. 2003;14(17):1595-1604.
- Von Seggern DJ, Kehler J, Endo RI, Nemerow GR. Complementation of a fibre mutant adenovirus by packaging cell lines stably expressing the adenovirus type 5 fibre protein. *J Gen Virol*. 1998;79(Pt 6):1461-1468.
- Greig JA, Buckley SM, Waddington SN, et al. Influence of coagulation factor x on in vitro and in vivo gene delivery by adenovirus (Ad) 5, Ad35, and chimeric Ad5/Ad35 vectors. *Mol Ther*. 2009;17(10):1683-1691.
- van Rooijen N, Kors N, Kraal G. Macrophage subset repopulation in the spleen: differential kinetics after liposome-mediated elimination. *J Leukoc Biol*. 1989;45(2):97-104.
- Koizumi N, Yamaguchi T, Kawabata K, et al. Fiber-modified adenovirus vectors decrease liver toxicity through reduced IL-6 production. *J Immunol*. 2007;178(3):1767-1773.
- Hamid O, Varterasian ML, Wadler S, et al. Phase II trial of intravenous CI-1042 in patients with metastatic colorectal cancer. *J Clin Oncol*. 2003;21(8):1498-1504.
- Small EJ, Carducci MA, Burke JM, et al. A phase I trial of intravenous CG7870, a replication-selective, prostate-specific antigen-targeted oncolytic adenovirus, for the treatment of hormone-refractory, metastatic prostate cancer. *Mol Ther*. 2006;14(1):107-117.
- Raper SE, Yudkoff M, Chirmule N, et al. A pilot study of in vivo liver-directed gene transfer with an adenoviral vector in partial ornithine transcarbamylase deficiency. *Hum Gene Ther*. 2002;13(1):163-175.
- Au T, Thorne S, Korn WM, Sze D, Kim D, Reid TR. Minimal hepatic toxicity of Onyx-015: spatial restriction of coxsackie-adenoviral receptor in normal liver. *Cancer Gene Ther*. 2007;14(2):139-150.
- Zhang Y, Chirmule N, Gao GP, et al. Acute cytokine response to systemic adenoviral vectors in mice is mediated by dendritic cells and macrophages. *Mol Ther*. 2001;3(5 Pt 1):697-707.
- Mebius RE, Kraal G. Structure and function of the spleen. *Nat Rev Immunol*. 2005;5(8):606-616.
- Alemaym R. Cancer selective adenoviruses. *Mol Aspects Med*. 2007;28(1):42-58.
- Shashkova EV, May SM, Doronin K, Barry MA. Expanded anticancer therapeutic window of hexon-modified oncolytic adenovirus. *Mol Ther*. 2009;17(12):2121-2130.
- Vigant F, Descamps D, Jullienne B, et al. Substitution of hexon hypervariable region 5 of adenovirus serotype 5 abrogates blood factor binding and limits gene transfer to liver. *Mol Ther*. 2008;16(8):1474-1480.